Improved Calculations of the Electronic and Nuclear Energy Loss for Light Ions Penetrating H and He Targets at Interrnediate Velocities

Pedro Luis Grande
Instituto de Física, Universidade Federal do Rio Grande do Sul
Bento Gonçalves 9500, Porto Alegre, RS, Brasil

Gregor Schiwietz
Hahn-Meitner-Institut GmbH, Department FD
Glienicker Str. 100, Berlin, Germany

Received January 25, 1994; revised manuscript received March 21, 1994

A review is given on the use of the coupled-channel method to calculate the electronic and nuclear energy loss of ions penetrating the matter. This first principle calculation based on an expansion of the time dependent electronic wavefunction in terms of atomic orbitals lias been applied to evaluate the impact parameter dependence of the electronic energy loss, the stopping cross-section and the fluctuation in energy loss of ions colliding with H and He atoms at energies of 10keV/amu to 500keV/amu. The results have been compared to experimental data as well as to others existing models e.g., local density approximation in an electron gas target, harmonic oscillator target treatment and first order plane-wave-Born approximation.

I. Introduction

During the last years many improved treatments of the energy loss of ions penetrating the matter have been presented in the literature. For solid targets the use of the density functional theory to describe the interaction potential between the incoming ion and the solid valence electrons has proven to be an efficient method to calculate the electronic stopping power for low-energy ions[1,2]. For high-energy bare ions colliding with gas targets, the stopping power as well as the impact parameter dependence of the electronic energy-loss have been calculated through the first-order perturbation theory[3,4] without using additional approximations, e.g. dipole approximation. At the same time, new insights have been achieved in the investigation of the electronic energy loss in an analytic harmonic oscillator treatment up to third order perturbation theory[5,6]. Nevertheless, presently two very important problems concerning ions penetrating the matter are of increasing interest. One is how to predict the behavior of the electronic stopping power at intermediate velocities near the stopping power maximum and how to obtain its impact parameter dependence.

At low and intermediate velocities most theories fail in the description of electronic energy transfer processes. Only theories which go beyond perturbation theory are applicable in this velocity regime. Specially there is no theory which accurately describes the low energy stopping processes for ions in gases or insulators. For this reason most of the stopping power tabulations[7–9] and semi-empirical models[10] extrapolate their results from intermediate and high energies to lower ones using velocities dependencies which are based on extremely simple models[11,12]. In the low velocity regime the energy loss is basically dominated by electron capture and loss of projectile electrons and, in the case of metals, due to the excitation of a small por-

tion of electrons near the Fermi level to empty states in the conduction band. According to the Firsov model[11] and Lindhard electron gas theory[12], both mechanisms yield a linear dependence of the electronic stopping power with the projectile velocity. For metals, this behavior is well corroborated by other calculations[13,14] and is a consequence of the minimum energy transfer being zero in these cases. On the other hand, in the case of gases or insulators, the electronic stopping power should fall off faster at low ion velocities, since in most cases there is a non-zero minimum energy transfer.

Besides the stopping power and energy straggling information, in some cases it is necessary to go deeper into the details of the energy loss phenomena. In particular, channeling experiments and measurements of energy Ioss as a function of scattering angle demand the knowledge of the impact parameter dependence of the electronic energy loss. Moreover, the full impact parameter dependence of the energy loss is a basic quantity to describe spatially correlated collisions that play an important role in structured targets, e.g. crystalline solids and diatomic gases. There are few descriptions of the average energy loss as a function of the impact parameter in the literature. Most of those models adopt either first-order perturbation theory[3,15,16] or local density approximation in an electron gas treatment of the target[17–20] or other approaches[11,21] in which it is hardly possible to determine the uncertainty due to the approximations involved.

Only recently some effort has been done in order to attack the stopping power problem starting from first principles in a non-pertubative way[22–26]. In this treatment, the electronic and nuclear energy losses are obtained by solving the electronic time dependent Schroedinger equation coupled with the classical motion of the nucleus through the coupled-channel method. These time-consuming calculations serve not only as a benchmark test for other models but also allow for an accurate determination of the importance of different processes leading to the energy loss of ions in gases or insulators. This full calculation accounts for the basic stopping processes in gases, namely electron capture and loss of projectile electrons as well as target ionization/excitation for different charge states of the incoming ion. The first stopping power calculation of this type was performed for the H^+ charge-state fraction at intermediate and high energies[22–24] and was later extended by including one projectile-centered state in order to improve the treatment of the capture process which is fundamental for the electronic stopping power at low energies[25]. For the first time it was possible to calculate the electronic stopping power of protons on He atoms with high accuracy.

In the present work we give a review on the coupled-channel method[22–26] applied to energy loss calculations. In the following, we shall give a brief description of the theoretical procedure used to describe the electronic and nuclear energy-transfer processes of light ions in H and He gases. In section III we discuss our numerical results for the impact parameter dependence of the electronic energy loss in connection with others energy loss models. In section IV, the results for the equilibrium mean stopping cross section are presented and compared to experimental data. We provide a comparison in section V of the calculated energy loss straggling results with some existing experiments. Finally, in section VI, we analyze the influence of the electronic energy-loss processes on the nuclear stopping power. If not indicated otherwise atomic units (a.u.) will be used throughout this paper.

II. Theory

Only few stopping-power models start from a detailed microscopic description of the electronic states in gases or solids[3,13,29]. In the case of solids, it is usually assumed that inner-shell excitations can be treated quite well as localized atomic events. It was shown on general theoretical grounds in refs. [26,27] that all high energy excitations (inner- and outer-shell ionization) in solids may be treated using atomic-collision models[3,30] and that a free-atom model is sufficient to describe energy losses in solids for incident energies above $\sim$ 10 keV/u, even when the energy loss is dominated by conduction-band electrons. However, it should be kept in mind that the charge-state distribution as well as projectile-screening effects differ between gas-targets and solids. This might lead to significant phase effects for the electronic stopping power (even for inter-band contributions)[29]. For intra-band transitions and low-energy inter-band transitions, however, the situation is more complicated. Calculations considering the full crystalline structure like the ones of refs.

[13,26,28] rnust be taken into account. Here we will focus attention on atomic treatments of the energy transfer process putting aside intra-band transitions and collective excitations such as bulk and surface plasmons in solid targets.

In a full quantum mechanical description, the ion-atom collision process is described by the many-body Schroedinger equation. For incident energies above a few eV/a the motion of the heavy particles may be described by classical nuclear trajectories $\vec{R}(t)$[31]. Then the electronic system obeys the time dependent Schroedinger equation[31]

$$H_e(\{\vec{R}(t)\})\Phi_e(\{r\},t) = i\frac{\partial}{\partial t}\Phi_e(\{\vec{r}\},t) \qquad (1)$$

where $\{\vec{r}\}$ represents all electronic coordinates and $\{\vec{R}(t)\}$ is the set of projectile and target nuclear coordinates. The nuclear trajectories may be obtained dynamically for each impact parameter b and each time t through the classical Hamilton equations for an averaged heavy-particle Hamiltonian[22] or, as in most current theories, they are simply replaced by straight lines.

The electronic many-body Hamiltonian in eq.(1) is treated in the framework of the independent-electron frozen-core model. This means that there is only one active electron, whereas the other electrons are passive (no dynamic correlation is accounted for) and no relaxation occurs. In this model the electron-electron interaction is replaced by an initial-state Hartree-Fock-Slater potential[32]. This treatment is expected to be highly accurate for heavy collision systems at intermediate to high incident energies and for $H^+ + H$ the treatment is exact (except for numerical uncertainties, relativistic effects and the classical heavy-particle motion discussed above). The largest uncertainties of the independent-electron model will show up for low-Z few-electron systems, such as H+H and H+He.

Furthermore, the independent-electron approximation allows for a distinction of target electrons and projectile-centered electrons which screen the projectile nuclear charge. One of the most important dynamic correlation effects (deviations from the independent-electron approximation) is the scattering of a target electron with a projectile-centered electron[33,34]. This will directly enhance the energy loss and reduce the projectile screening. Similar fluctuations of the screened projectile potential can be due to the interaction with the target potential. These fluctuations might strongly increase the stopping cross-sections and are not accounted for in any of the present theories for the stopping of low energy ions in metals. It follows that a separate treatment of the different projectile charge states is important for reliable predictions of the mean energy loss for atomic targets[3,22–26,30,33], insulators and, at higher incident energies, also for metals[29,35,36].

The time-dependent Schroedinger equation may be solved by expanding $\Phi_e(\{\vec{r}\},t)$ in terms of unperturbed eigenfunctions ϕ_i of the target and/or the projectile with coefficients $a_i(t) = <\phi_i|\Phi_e(t)>$. Thus, eq.(1) is replaced by a set of coupled first-order differential equations, the so-called coupled-channel equations:

$$i\frac{d}{dt}a_i(t) = \sum_j a_j(t)e^{i\omega_{i,j}t}V_{j\to i}(\{\vec{R}(t)\})\ \omega_{i,j} = E_i - E_j \qquad (2)$$

with the internuclear distance $\vec{R}$ and

$$V_{j\to i}(\{\vec{R}(t)\}) = <\phi_i|V_p(\vec{R}(t),\vec{r})|\phi_j>\ , \qquad (3)$$

where E_i is the orbital energy associated with the target wavefunction ϕ_i. Here V_p is an effective potential seen by the active electron, and contains the screening effect produced by other electrons from the medium. For bare incident ions, the active-electron projectile interaction V_p is just the Coulomb potential. However, in the case where the projectile carries electrons, we use the hydrogen-like screened potential

$$V_p(\vec{R}-\vec{r}) = -\left(\frac{Z_p - n_p}{|\vec{R}-\vec{r}|} + n_p\left(Z_{eff} + \frac{1}{|\vec{R}-\vec{r}|}\right)e^{-2Z_{eff}|\vec{R}-\vec{r}|}\right) \qquad (4)$$

where Z_p is the projectile nuclear charge, n_p is the number of projectile electrons and Z_{eff} is the effective projectile charge as seen by the electrons which are attached to the incident ion. It is pointed out, that

the dynamic interaction between the bound projectile electrons and the target electrons is not included in the present model. The corresponding effect results in an enhancement of the ionization and excitation cross-sections at high incident energies (dynamic screening) and at intermediate energies (antiscreening)[37,38].

Considering the angular and radial parts of the atomic target-centered wavefunction ϕ_i, we have evaluated the matrix elements **(3)** using the multipole expansion

$$V_p^{i,j}(\vec{R}) = -\sum_{L=|l_i-l_j|}^{l_i+l_j} W_{L,M}^{i,j} G_L^{i,j} Y_{L,M}(\hat{R}), \quad M = m_j - m_i \tag{5}$$

with

$$W_{L,M}^{i,j} = \left(\frac{4\pi(2l_i+1)(2l_j+1)}{2L+1}\right)^{1/2} (-1)^{m_i+M} \begin{pmatrix} l_i & l_j & L \\ 0 & 0 & 0 \end{pmatrix} \begin{pmatrix} l_i & l_j & L \\ -m_i & m_j & -M \end{pmatrix}, \tag{5a}$$

and

$$G_L^{i,j}(R) = \int_0^\infty dr r^2 \chi_i^* \chi_j f_L(r,R), \tag{5b}$$

where

$$f_L(r,R) = Z_p \frac{r_<^L}{r_>^{L+1}}, \tag{5c}$$

for an unscreened projectile. In the case of a screened projectile given by (4), $f_L(r,\mathrm{R})$ reads

$$f_L(r,R) = (A_L(\lambda r_<) H_L(\lambda r_>) - \lambda(r_< A_L'(\lambda r_<) H_L(\lambda r_>) + r_> A_L(\lambda r_<) H_L'(\lambda r_>)))$$

$$\times (2L+1)(-1)^L \frac{\lambda n_p}{2} + (Z_p - n_p)\frac{r_<^L}{r_>^{L+1}}, \tag{5d}$$

with $\lambda = 2Z_{eff}$ and $A_L(x) \equiv \mathrm{i}^L \mathrm{j}_L(\mathrm{ix})$ and $H_L(x) \equiv i^{L+1} h_L^+(ix)$ are related to modified spherical Bessel functions[39]. The notation $r_{<(>)}$ means the smallest (largest) of the values of r and R. l and m are the quantum numbers associated with angular momentum and angular momentum projection and χ_i, χ_j are the radial wavefunctions of the states i and j respectively. The symbols $\begin{pmatrix} \cdots & \cdots & \cdots \\ \cdots & \cdots & \cdots \end{pmatrix}$ in eq. (5a) represent the Wigner 3j-symbol as described in ref. [39].

The essence of the present calculation is to solve numerically in time, step by step, Eq.(1) and the classical trajectory of the nucleus in order to obtain the coefficients a_i after the collision ($t = \infty$), since the probability of exciting (or ionizing) the active electron from the target in a collision with impact parameter $b(P_i(b))$ is given by:

$$P_i(b) = \lim_{t\to\infty} |a_i(t)|^2 \tag{6}$$

The probability $P_i(b)$ should be highly accurate as long as electron capture by the projectile is of minor importance. The description of even a single projectile state requires an infinite number of single-centered target states as basis set. Therefore, in the case of a bare projectile, a hydrogenlike 1s projectile-centered state is also included

$$\phi_p(\vec{r} - \vec{R}, t) = \frac{2}{\sqrt{4\pi}} Z_p^{3/2} \mathrm{e}^{Z_p|\vec{r}-\vec{R}|} e^{i\vec{v}\cdot\vec{r}} e^{-i\epsilon_p t}, \tag{7}$$

where $\vec{R}$ and $\vec{v}$ are the relative coordinate and velocity between projectile and target nucleus respectively. ϵ_p is the sum of the internal energy of the projectile-centered state and the translational energy $\frac{1}{2}v^2$. This extra state strongly improves the stopping power calculation at low energies since capture into the projectile-excited states

is of minor iinportance. It should be pointed out that the above projectile-centered state is preorthogonalized in the present calculation by subtracting its projection on all target-centered states[40].

The matrix elements between target-centered and projectile-certered states are calculated by replacing the translatic n factor $\exp(i\vec{v}\cdot\vec{r})$ by its Taylor expansion up to the second order around $\vec{R}$. This is well justified at low velocities since $\vec{v}\cdot\vec{r}$ varies sufficiently slow in the region where ϕ_p is most important. This low-energy approximation is very useful, because the use of exact velocity dependent matrix-elements would be very time consuming and the electron capture contributions are only important for low to intermediate velocities. It is emphasized that a Taylor expansion around the mean value of $\vec{r}$, as it was used in previous works[40], leads to problems for transitions between the projectile state and the target continuum.

Each excited or continuum state corresponds to a well defined energy transfer $\Delta E_i(= E_i - E_0)$. Then the average electronic energy loss $\bar{Q}(b)$ in a given impact parameter b can be written as:

$$\bar{Q}(b) = \sum_i P_i(b)\Delta E_i \ . \tag{8}$$

The electronic stopping power S_e and energy straggling W per atom can be computed directly from

$$S_e = \sum_i \sigma_i \Delta E_i \ , \tag{9}$$

$$W = \sum_i \sigma_i \Delta E_i^2 \ , \tag{10}$$

where

$$\sigma_i = \int_0^\infty 2\pi b db P_i(b) \tag{11}$$

is the cross section for excitation (or ionization) from the ground-state to a state i. It is noted that the above sums have tc be replaced by integrals in the case of continuum states.

The corresponding atomic-orbital (AO) expansion includes the binding effect and polarization in a natural way. Additionally, electron capture is accounted for and the norm is preserved. This means that the sum over the population probabilities of all states is always equal to one in the AO model, unlike as in perturbative approaches. In the latter approaches even for $H^+ + H$ collisions the total ionization probability may exceed one.

In this work we are only interested in electronic energy loss processes. However, the kinetic energy transferred from the ion to the target core, the nuclear stopping process, can be obtained directly from the calculated classical trajectories.

We can also restrict the present computer code to the so-called SCA, Semi Classical Approximation[3,41]. In this approach, the nuclear trajectories are assumed to be straight lines and the coupled-channel equations are solved by neglecting all matrix elements, except those which lead to transition from initial state, $1s$ (or $1s^2$ in He case), to one of the final states. This model yields the same cross section as the first-order- Plane-Wave-Born-Approximation (PWBA)[42].

It was verified that the coupled-channel results agree with the predictions of the first order perturbation theory (SCA) in the case of a small perturbation. Small perturbations correspond to either fast projectiles, large impact parameters or small projectile charges. Thus, the advantages of coupled channel calculations compared to first order theories should show up especially at intermediate incident energies and for small impact parameters. In contrast to other coupled-channel calculations we have used a large number of continuum wave-packets that are composed out of a superposition of continuum eigenstates (up to **350** gerade states with partial waves up to $l = 8$), since the computation of the stopping power demands high accuracy of the emitted electron energy spectrum. In addition, the energy loss due to capture into projectile excited states is naturally included in a large-basis-set calculation.

Further details of the calculation, e.g. the numerical treatment of continuum states and adopted basis set, may be found in ref. [22].

III. Impact parameter dependence

The numerical results for the impact parameter dependente of the energy loss calculated according to the last section are presented in Figs. 1-4. Fig. 1 shows the energy dependence of the electronic energy loss for protons incident on He. For impact parameter smaller thari 2 a.u the shape of $\bar{Q}(b)$ is approximately described

by an exponential $e^{-\alpha b}$ function (dashed line). In fact, this behavior was found for almost all cases studied by us. In addition we have found that the coefficient a depends only weakly on the projectile energy. For protons (E > 20 keV) on H, $a \approx 0.9$ and for p on He, $\alpha \approx 1.4$. For lower energies, the energy loss $\bar{Q}(b)$ cannot be described by an exponential function anymore. As a ansatz, the exponential behavior of the impact parameter dependence of the electronic energy loss was already proposed by Oen and Robinson[43]. They have suggested that the α parameter, which deviates from our results, is a function of the interatomic screening length and independent of the projectile energy. At larger impact parameters (> 3 a.u.), however, tlie shape of $\bar{Q}(b)$ depeiids strongly on the incident energy.

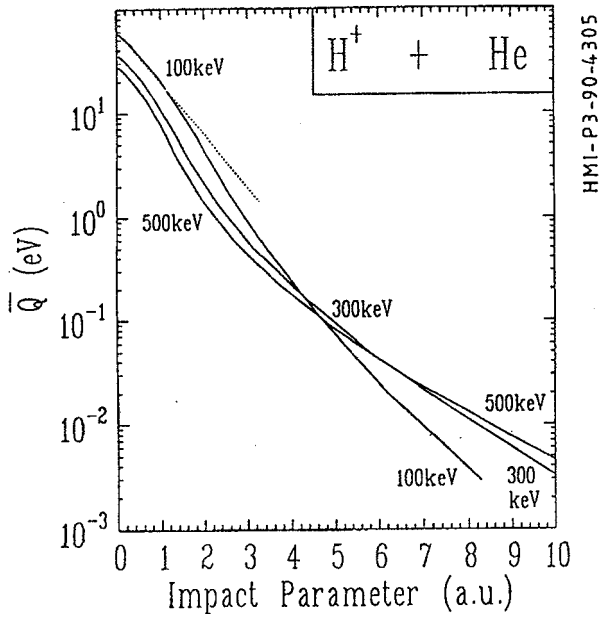

Figure 1: Theoretical results of the mean electronic energy loss for proton incident on He at 100, 300 and 500keV. Dashed line represents an exponential curve with $\alpha = 1.2$ (see text).

From Fig. 1 we can also observe that the curves become flatter at large impact parameters with increasing ion energy. This is in agreement with the result of first order perturbation theories[44], where it is known tliat the mean impact parameter for excitation and ionization processes is proportional to the ion velocity v_p. It is emphasized that the contribution due to excitation becomes dominant at large impact parameters. We can also note that $\bar{Q}(0)$ follows the energy dependence of the electronic stopping power, and shows a maximum around 80 keV [22].

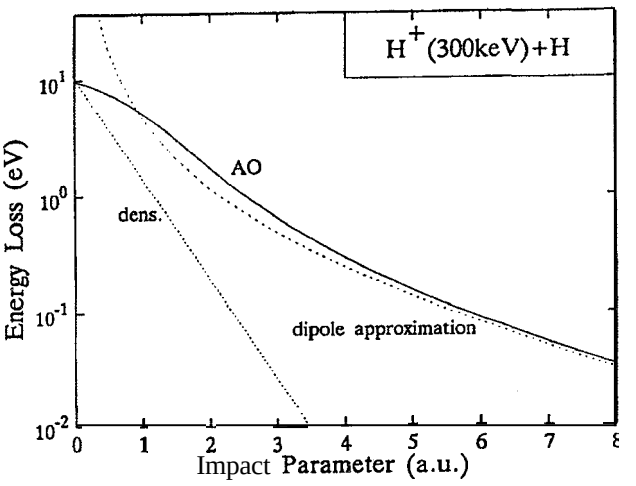

Figure 2: Comparison between our theoretical result of $\bar{Q}(b)(AO)$ for $H^+ + H$ collisions at 300keV with different models: i) The electronic energy loss is proportional to the electronic density integrated along the ion trajectory (dens.); ii) Classical Bohr energy-loss formula[45] with ω = 0.5a.u. (dipole approximation).

In Fig.2 the calculated impact parameter dependente of the electronic energy loss for protons on H at 300keV is displayed. The dotted line represents a simple inodel where it is assumed that the energy loss is proportional to the electronic density integrated along the ion path. In fact, compared to the electronic density of the target atom the energy loss $\bar{Q}(b)$ falls off very slowly. This tendency, indicating a break-down of the local density model, was observed for all cases (H and He targets). For large impact parameters our numerical results are quite well described by the Bohr's classical oscillator model[45] with a frequency $w = 0.55$. Tlie classical energy-loss formula[45], when generalized to an ensemble of harmonic oscillators, is equivalent to a quantum-meclianical calculation in the first-order perturbation theory using the dipole approximation. Both approximations are meaningful for large impact parameters.

Fig. 3 displays the present calculation for 300 keV $H^+ + He$ collisions in comparison with others $\bar{Q}(b)$ modeis existing in the literature. The models (O-1)and (0-2) correspond to the first and second order quantum perturbation theory in a harmonic oscillator target respectively, as proposed by Mikkelsen and Sigmund[5,6] witli two harmonic oscillators of the same frequency

w = 1.54 a.u.[6]. In this model a near gaussian dependente of $\bar{Q}(b)$ is predicted for smaller impact parameters, iri contrast to the exponential shape found for realistic target wavefunctions. However, the overall agreement with our results is reasonable. In this figure, the mean energy transfer is also evaluated by using a local-density electron-gas treatment (LDA)[20] and the agreement with the AO calculation is not good. In fact, for the present case of atomic transitions (or interband transitions), the applicability of such a model (neglect of the target level-structure) is rather dubious. A breakdown of the local density model was observed for ali cases (H and He targets at different incident energies). This finding is very important, since most of the energy loss models used for the description of channeling are based on the assumption that the electronic stopping power depends only on the local electron density. As shown in ref. [13], however, this assumption is reasonable for intra-band transitions in metals.

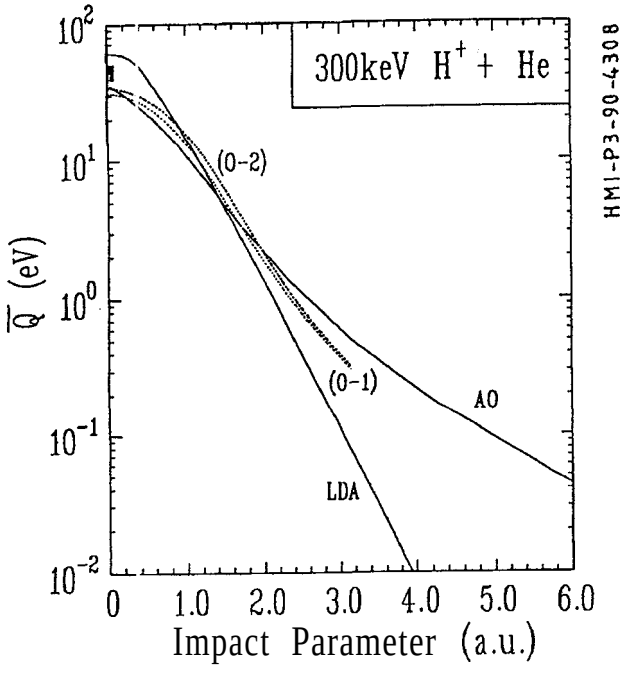

Figure 3: Theoretical mean energy loss as a function of impact parameter for 300keV $H^+ + He$ coliisions. Present theory is denoted by (AO). Dashed lines (0-1) and (0-2) correspond to a calculation of $\bar{Q}(b)$ in a harmonic oscillator target with w = 1.54 a.u. from refs. [5,6] approximation in a electron gas target[15]. He($1s^2$) ground-state density was used. The experimental point in b=0.02 was taken from ref. [46].

One experimental data point from ref. [46] is also presented for b = 0.02 a.u.. The agreement of this data point with the AO result in Fig. 3 is good and a similar good agreement was found for the energy spectrum[47] as well as for the angular distribution[46] of ejected electrons in $H^+ +$ He collisions. However, a much better agreement can be achieved by increasing the size of the basis set or adapting the basis set to the physical situation[22,46]. For small irnpact parameters, only states with angular momentum projection numbers m = 0 need to be considered. It should also be pointed out that double ionization processes become important for He target mainly for very small impact parameters and that the present calculations can not properly take into account these processes because of the independent electron model which was employed in the calculations.

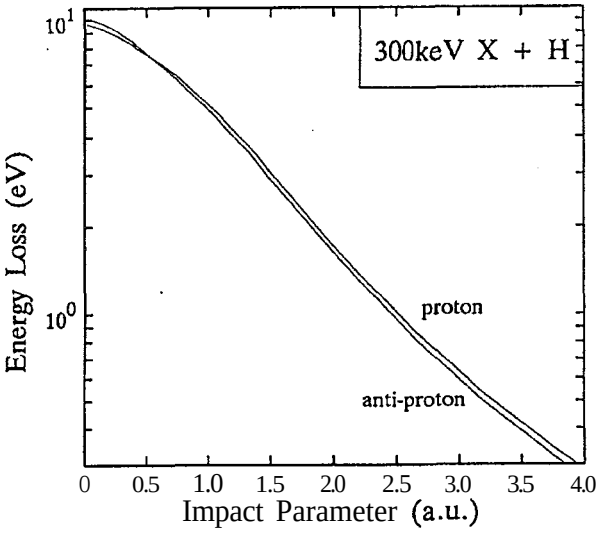

Figure 4: Electronic energy loss as a function of impact parameter for p and p penetrating atomic H at 300keV.

The impact parameter dependence of the electronic energy loss for protons and antiprotons on H at 300 keV is shown in the Fig. 4. In contrast to a first order calculation where the excitation and ionization probabilities are proportional to Z_p^2, the squared projectile charge, Fig. 4 displays a behavior different for incident p and p. For large impact parameters this difference comes from the polarization effect, which is not included in first order (SCA) calculation. The projectile can attract or repel the electrons, depending on its sign of charge. This implies an enhancement or reduction of the electronic density around the projectile trajectory and consequently, of the electronic energy loss. For small impact parameters the presence of the projectile

charge may increase or decrease the electron binding energy. This binding effect can enhance or reduce the probability to excite or ionize the target electron. It always Peads to a significant reduction of the polarization effect.

IV. Electronic stopping power for light systems

Fig. 5a shows our coupled-channel (Atomic Orbital) results for the electronic stopping cross sections corresponding to hydrogen beams penetrating He gas. In order to calculate the equilibrium mean stopping power we must consider the charge state distribution of the projectile and the fact that we are restricted to only one active electron. Then, we have to calculate the energy loss in 3 reaction classes:

1) $H^+ + He^0 \rightarrow H^+ + He^*$ or $\rightarrow H^0 + He^+$

2) $H^0 + He^0 \rightarrow H^0 + He^*$

3) $He^0 + H^0 \rightarrow He^0 + H^*$

where * includes excitation and ionization as well. For case 1 we have evaluated the electronic energy loss due to the electron capture process. Ionization and excitation of the target electrons have been computed for 1 and 2. Case 3 provides the energy dissipation by projectile electron loss and projectile excitation. The energy loss involving neutral collision-partners ($H^0 + He$ and $He + H^0$) is basically due to target or projectile ionization. Excitation of the target or the projectile is of minor importance. The same holds true for collisions between H^+ and He at high energies (E >100 keV). However, the main contribution for low energies comes from the capture of target electrons into the projectile 1s state. From Fig. 5 we can see that the partial electronic stopping power for bare hydrogen is dominant at high energies whereas excitation and ionization of the projectile yield the highest partial cross section at low velocities. Nevertheless, the projectile ionization leads to an enhancement of the H^+ charge-state fraction and consequently the contribution of H^0 to the stopping processes is reduced. The experimental equilibrium fractions[48] for hydrogen beams in He gas are shown in Fig. 5b. The H^+ fraction increases for high and low energies as well. The neutral fraction is only significant for intermediate ion velocities. This means that the $H^+ + He$ collisions also dominate the low energy part of the stopping power. For energies around 30keV/u, all reaction classes are equally important.

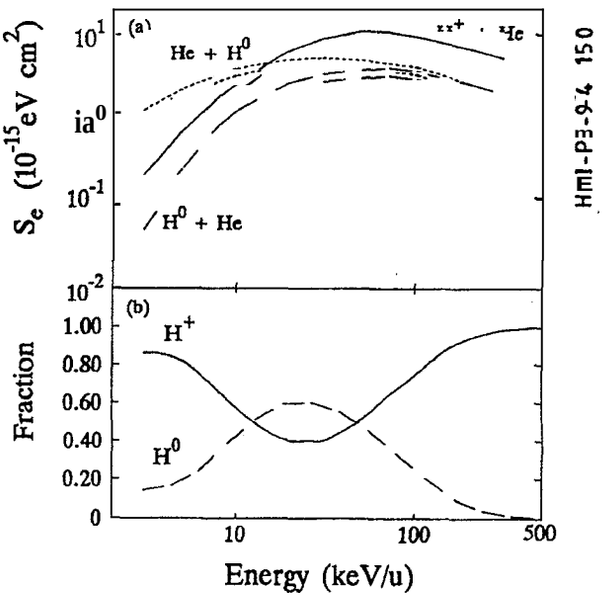

Figure 5: a) Coupled-channel results for electronic stopping cross section for H^+ and H^0 incident on atomic He versus incident energy (solid and long-dashed lines). Ionization and excitation of the projectile, in the case of the H^0 charge-state fraction is accounted for by considering the coliision system $He + H^0$ (short-dashed line). b) Experimental equiiibrium fractions for hydrogen beams in helium gas from ref [48].

It is pointed out that we could not estimate the equilibrium fractions of H^+ and H^0 from the present calculation at high energies because of the above described approximation (Taylor expansion) which is involved in the computation of the capture matrix elements. In fact, the low energy Taylor-expansion works quite well only for energies lower than 20keV/u. This is not a problem, since, for high energies, it is possible to evaluate the total energy loss due to capture and ionization employing a huge basis set[24].

In Fig. 6 the equilibrium mean total stopping cross section per atom for H + He collisions is presented in comparison with experimental data of different groups[49–53]. The solid curve represents the values of Fig. 5a weighted with the corresponding charge-state fractions from Fig. 5b (the contribution due to H^- can be neglected[48]). For comparison, we have added the ZBL nuclear stopping power[10] for incident deuterons (at low velocities the experiments were carried out with deuterons) to our calculated values. Nevertheless, according to ref [10], the nuclear stopping contribution is much less than 3% for energies higher

than 8 keV but can reach 30% at 3 keV. Special attention should be drawn to the low energy stopping power data which was recently measured by Golser and Semrad[54]. At energies below 10keV experimental and theoretical results agree within 5% or better.

At 30 keV/u we find the largest deviation between the measurei stopping power and our calculated values of about 12%. This may be attributed to an overestimation of cross-sections for multi-electron processes because of the use of the independent particle model[46]. We emphasize that the present calculation does not properly take into account events in which more than one electron is actively involved, e.g. double target ionization or excitation and simultaneous projectile and target ionization.

Fig. 7 cisplays the equilibrium mean total stopping cross-section per atom for $H + H_2$ collisions in comparison with experimental data of different groups[49–53 55–57]. The solid curves represent AO results for incident protons and hydrogen atoms (the contribution due to H^- can be neglected[48]) on (atomic) H targets we ghted with the corresponding charge-state fractions[48]. There is also a very good overall agreement between the A 0 results and the experimental data. At low as well as at high incident energies the agreement is generally better than 4% (which is about the experimental uncertainty). At 55 keV/u we find the largest deviation of about 6% between the measured stopping power and our calculated values. This deviation is slso attributed to the influence of multi-electron processes because the AO theory relies on the independent-electron model. The target double target-ionization (for the H_2 molecule) (a part of the dissociation processes) is expected to be of minor importance. But in this case we underestimate the simultaneous projectile and target ionization in $H^0 + H_2$ collisions. Correlated two-e'ectron transitions come into play at energies above 30 keV. An estimated value (relying on perturbation theory) for the corresponding contribution is shown as a solid arrow in the lower part of Fig. 7. The corresponding enhancement of the mean stopping cross section will, however, be partly canceled by the influence of the increased binding energy in H_2 compared to atomic hydrogen. An estimate for the reduction of electron loss, target ionization and electron capture is shown as a dashed arrow. Molecular as well as multi-electron corrections are expected to be less than 1%at energies above 200 keV.

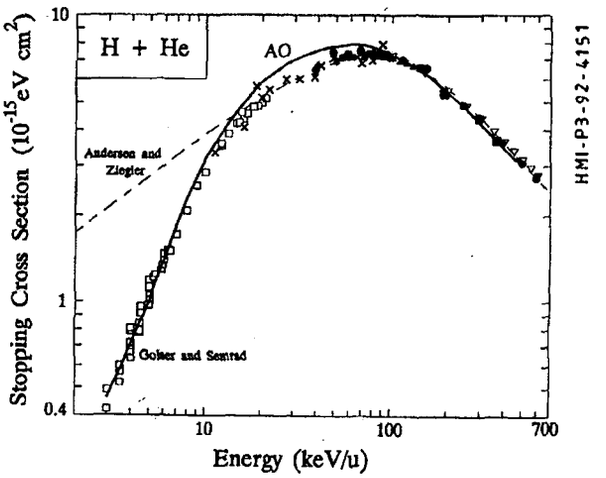

Figure 6: Equilibrium mean stopping cross section per atom for hydrogen beams penetrating He gas. Theoretical results: present atornic orbital (AO) calculation (solid line), Andersen and Ziegler[8] (dashed line). Experimental values: open triangles[49], crosses[50], closed squares[51], closed triangles[52], closed circles[53], open squares[54].

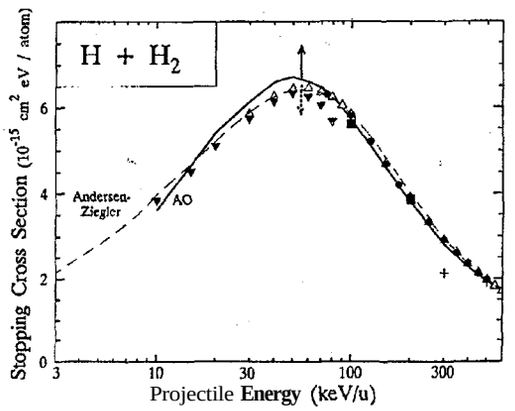

Figure 7: Equilibrium mean total stopping cross-section per atom for H + H_2[18] collisionç as function of the incident energy. The solid curves represent AO results in comparison with experimental data of different groups. Experimental values: closed triangles[50], open triangles[49], closed circles[56], closed squares[55] and crosses[57]. The arrow indicates the maximum contribution due to the electron-electron interaction in $H^0 + H^0$ collisions. The dashed lines correspond to the semi-empirical formula by Andersen and Ziegler[8].

The Figs. 6 and 7 display also the electronic stopping power as predicted by the fitting formula of Andersen and Ziegler[8] who use velocity proportionality to extrapolate their fit down to low energies. The deviation from the velocity proportionality was assigned

in ref. [54] to a threshold effect, i.e., the existence of a finite minimum energy transfer in H + He collisions. According to our calculations, the low energy part of the stopping power is governed by electron capture which has a minimum energy transfer $\Delta E_{\min}$ of about $(0.4 + 0.5v^2)$ a.u.. A useful criterion may be given to determine the threshold projectile-energy E_t below which the effect of a minimum energy transfer $\Delta E_{\min}$ becomes important. If we suppose that the maximum energy-transfer between projectile and electron in a binary collision should exceed $\Delta E_{\min}$ we have $E_t = M_p \Delta E_{\min}/4$ (M_p is the projectile mass in units of electron mass). Using this criterion we estimate a classical threshold energy of 8 keV which is consistent with Fig.7. Furthermore, for the investigated case of $Z_p < Z_T$ and $I_p < I_T$ (I_p and I_T are the projectile and target ionization potentials, respectively) the electronic stopping cross section Se may be approximated by

$$S_e \approx \sigma_{\text{capture}}(I_T + v^2) \,, \tag{12}$$

at low velocities. The energy transfer $(I_T + v^2)$ accounts for a single capture-and-loss cycle of the q = 1 charge-state fraction. For homo-nuclear systems $(Z_p = Z_T)$ at low energies one may write

$$S_e \approx \sigma_{\text{loss}}(2I_T + 1.5v^2) + 2\sigma_{\text{excitation}} \Delta E_{\text{excitation}} \,. \tag{13}$$

The corresponding cross sections σ_{loss} and $\sigma_{\text{excitation}}$ for neutral projectile and σ_{capture} for singly-charged ions may be obtained from tabulated atomic cross sections. It should be emphasized that Kimura[58] has recently performed a more complete analysis of this type for H + He and H + H_2 systems.

V. Electronic straggling calculation

The fluctuation in energy loss of a monoenergetic incident beam passing through matter is not only due to the energy loss variation in each individual collision, but also due to the statistical fluctuation in the number of collisions suffered by the penetrating ion. Assuming statistic independence of the collision events, the variance of the energy loss distribution (Q^2) can be calculated, for a thin penetrated layer Sx, as [45]:

$$\Omega^2 = N \delta x W \,, \tag{14}$$

where N is the target density (atm/cm^3) and W is given by Eq.(10).

For an extremely thin penetrated layer, the energy loss spectrum will exhibit a single collision energy loss structure. On the other hand, if much more collisions happen, the energy loss distribution will be broadened. If additionally the mean energy loss is much less than the initial projectile energy, the final energy loss distribution will tend to a gaussian profile[45]. According to Bohr[45], the straggling of a high velocity particle with atomic number Z_1 penetrating matter with atomic number Z_2 is given by

$$\Omega_B^2 = N \delta x 4\pi Z_1^2 Z_2 \,, \tag{15}$$

which is independent of the ion velocity v_p. In general, at low energies, the electronic straggling increases as a function of the projectile velocity.

The existing measurements of straggling in energy loss of H ions in gases were performed in an energy range where there are two equilibrated charge states of the projectile H^+ and H^0. Similar to the mean equilibrium stopping power calculation, an averaged straggling has to be taken into account

$$\Omega^2 = F_1 \Omega_1^2 + F_0 \Omega_0^2 \,, \tag{16}$$

where Ω_1^2, Ω_0^2 are the straggling in energy loss for the charge-state fractions F_0, F_1 for H^+ and H^0 respectively. These values may be found for H_2 and He targets in the review of S. Allison[48].

Special attention must be drawn to molecular gas target. According to Sigmund[59], the molecular geometry influences the spectral distribution of energy loss, deflection angles and excitation phenomena. From a purely geometrical point of view, disregarding the differences between the electronic states of the constituent atoms in a molecule and in a free atom, Sigmund obtained an adclitional positive definite term to the expression (14) for binary molecules:

$$\Omega_M^2 = N \delta x \langle \int d^2b \bar{Q}_1(b_1) \bar{Q}_2(b_2) \rangle_\Omega \,, \tag{17}$$

where the $\langle \ldots. \rangle_\Omega$ means an average over all possible orientations of target molecules, $\bar{Q}_i$ is the mean energy loss in a collision with target atom i of the molecule and b_i is the impact parameter relative to the i-atom. This correction was for the first time evaluated from a

realistic impact-parameter dependence in ref [23]. The straggling produced by charge-state fluctuation according to ref [60] was also estirnated. But for the present cases this effect is of rninor importance.

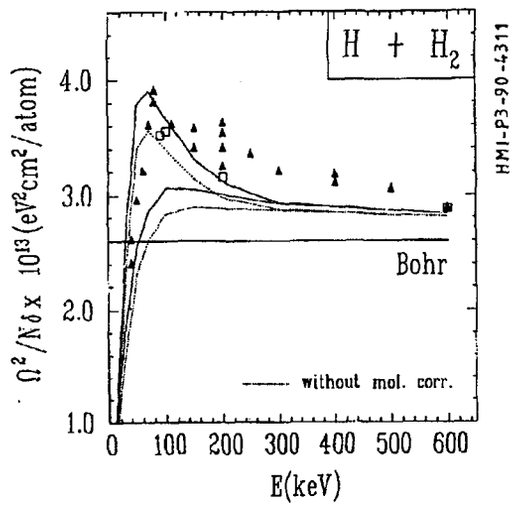

Figure 8: **Equilibrium mean total electronic straggling in energy loss pei atom for incident** H **in** H_2 **target in comparison with** e:xperimental **data from ref** [62] **(square) and ref** [61] (triangle). Solid **curves represent the calculation with the molecular term correction from** Eq.(18). **The difference** between **the two upper and lower curves is due to the treatment** r**sed to evaluate the excitation and ionization cross-sections** f:or $H^0 + H^0$ **collisions (see text).**

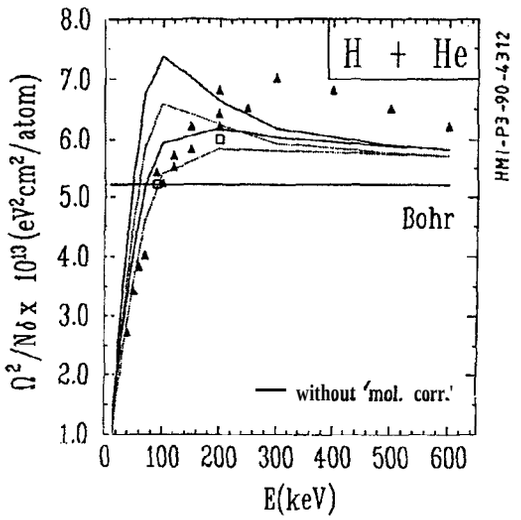

Figure 9: The s**ame as in Fig.** 8 **for incident H in He gas target.**

Figs. 8 and 9 show the present straggling calculation in comparison with experimental data[61,62]. The dashed lines ccsrespond to the evaluation without the molecular term (17). For the He target, it is also necessary to evaluste the molecular correlation term since we are assuming, according to the independent electron model, the He target as being two full overlapping "effective one electron atoms" each having the sarne one-electron wavefunction. It should be pointed out that for the first time this 'bunching effect',which was originally calculated by Besenbacher et al[60], is evaluated without using electron gas models[60].

The difference between the two upper and lower curves is due to the treatment used to obtain Ω_0^2 in (16). In our calculation, we have assumed the neutral projectile to act as a screened Coulomb potential, (lower curves), or we can take the dynamic motion of the projectile electron into account in PWBA calculations according to [38] . This implies, especially for srnall impact parameters, a so called antiscreening effect (upper curves). Nevertheless, the treatrnent described in ref [38] usually overestimates the excitation and ionization cross sections. Therefore, we expect that an exact two-electron treatment will yield a curve between the ones plotted as solid lines.

As can be observed frorn Fig. 8, for $E < 200$ keV the experimental points lie between the calculated values showing consistence of the theoretical results. But for the energy range between 200 and 600 keV, the theoretical predictions underestimate the experimental data by $\approx 10\%$. For these energies, there are basically only $H^+ \rightarrow H_2$ reactions and the molecular correlation term (17) is srnall. In principle, we did not find any reasonable explanation for this discrepancies. However, as can be seen from the scatter of the data points at $E = 200$keV, the experimental error seerns to be larger than 5-7%, as quoted in ref [61].

The same systematic deviation from the theory, for $E > 300$ keV, can be seen in Fig. 9, for the He target. In this case, the discrepancies are still higher (about 15%). For lower energies, the agreement is also not good. However, in this energy range, the dominant contribution to the electronic straggling comes from $H^0 +$ He collisions. Besides the problems which may emerge from the description of projectile ionization, we have used hydrogen like wave functions to describe the target excitation and ionization processes. It is well known that these functions deviate significantly from more sophisticated He target wave functions. It is emphasized, that the solid curves in Fig. 9, i e. "rnolecular

correlation", stand for an independent particle treatment of double ionization. The double-ionization probabilities are known to be overestimated by a factor of 6 in the independent particle model[46]. However it is not possible to determine from the existing experimental data the uncertainties due to approximations involved in our treatment.

VI. Nuclear stopping cross section

At low incident energies the nuclear stopping process determines the slowing down of ions in the matter. Calculation with parametrized time-independent potentials have yielded stopping powers and ranges in good agreement with experimental data[10] except for some special systems[63]. These potentials correspond to static (frozen) electronic charge distributions. However, investigations of highly charged ions or negative particles require the treatment of collisional excitation processes and of the resulting dynamic target polarization. Any polarization during the collision will influente the projectile/target interaction potential. Hence, the nuclear stopping power is changed. It should he emphasized that the nuclear stopping may also be influenced by the electronic energy loss in a different fashion for many-electron systems due to the formation of quasi-molecular orbitals that influence the excited potential[63].

We have used our atomic-orbital coupled-channel code to calculate dynamic curved projectile trajectories for protons and anti-protons in the field of polarized hydrogen atoms. According to section II the electronic motion is treated quantum mechanically resulting in a time-degendent electronic density. The nuclear motion is determined simultaneously by Newtow's classical equation of motion and the nuclear energy transfer may directly be extracted. Fig. 10 shows scaled nuclear energy loss cross sections for different incident light particles on atomic hydrogen. For fast projectiles the nuclear energy loss cross section S_n behaves roughly as the reciproca1 of the incident energy E_p and the maximum of S_n is at about 50 eV. Thus, $S_n * E_p$ shows an increase of only a factor 3 when E_p is varied from 1 to 300 keV. The lowest curve in Fig. 10 is the well-known ZBL stopping-power prediction[10]. It relies on an approximate treatment of the static interaction between a projectile and the target atom. Since both collision partners are screened, in this case the results are lower than the static results for incident protons and anti-protons. For anti-protons at low velocities the static results are slightly larger than for protons because the distance of closest approach r_0 is smaller for anti-protons.

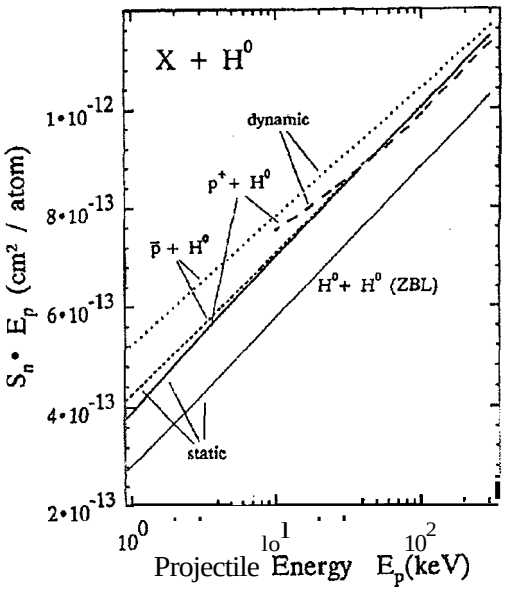

Figure 10: Scaled nuclear stopping power as a function of the projectile energy for protons (long-dashed and thick solid line), antiprotons (dotted and short-dotted lines) and neutral hydrogen incident on hydrogen atoms. Thin solid line: ZBL prediction[10] for neutral projectiles. For two of the curves (dotted and long- dashed) dynamic target polarization has been accounted for in the calculation

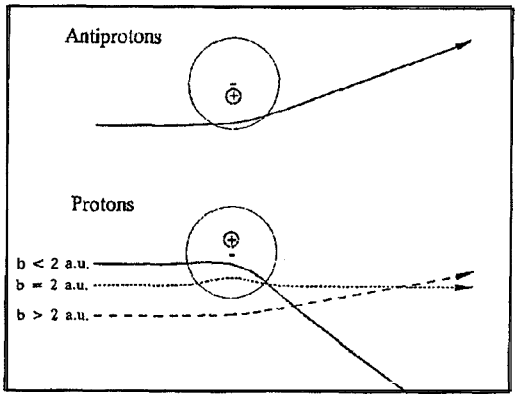

Figure 11: Scheme showing typical projectile trajectories of protons and antiprotons in the field of polarized target atoms.

Especially at low energies, the results of dynamic calculations show a significant deviation from the static

ones. At 1 keV the anti-proton results with polarization lie about 25% above the static results. Furthermore, S_n clearly shows a different energy dependence for anti-protons and protons. The reason for this deviation is clepicted in Fig. 11. At large impact parameters negative projectiles repel the target electron cloud and positively charged particles attract the electsons. Hence, in both cases the projectile is deflected towards the target atom and the deflection is larger than in the static case. The situation is different for the positive ions at small impact parameters: at larger internuclear distances the projectile is attracted by the electron cloiid, but at small distances the Coulombforce between the nuclei leads to a sudden projectile deflection away from the target nucleus. At low energies, this repulsion is even enhanced due to a reduction of r_0. At intermediate impact parameters, the attraction and the repulsion are of the same strength and the trajectory is nearly a straight-line. Thus, the nuclear energy transfer is strongly reduced and at a certain impact parameter it is even zero.

Finally, at low incident energies, larger impact parameters gain importance and the dynamic results exceed the static ones. On the contrary, for fast positively charged projectiles the zero-crossing of the projectile scattering angle (at about 2 a.u. in the case of H) leads to slight reduced dynamic nuclear stopping cross sections.

VII. Conclusions and outlook

Full calculations of the electronic stopping power are presented by considering, in detail, each basic single-electron mechanism of the energy loss of bare and neutral hydrogen atoms penetrating H and He gas targets. A good overitll agreement with experimental results of different groups was obtained and the remaining discrepancies of about 10% at intermediate energies are assigned to rnulti-electron processes. It is emphasized that these effects will be less important for heavier projectiles and targets, since the electron-electron interaction will be reduced in comparison with the nucleus-electron interaction. For very low incident energies we give scaling rules for the electronic stopping power in gases or insu ators that are based on atomic cross sections for electron capture and loss.

The impact-parameter dependence of the mean energy transfer was found to be consistent with the Oen-Robinson ansatz for $b < 2$ a.u. At larger impact parameters, however, the slope of the energy transfer curve depends significantly on the incident energy. Furthermore, local-density free-electron gas models clearly fail in the description of the impact-parameter dependence of the electronic energy loss at small as well as at large impact parameters.

The theoretical straggling values are in relatively good agreement (to within 10%) with the experimental ones. However, there is a need for more experimental data with'improved accuracy.

In conclusion, for atoms, insulators or inner shells of conductors accurate stopping cross sections may be computed (including excitation, ionization and electron capture) using the atomic-orbital (AO) coupled-channel method. This is very time-consuming, since it has to be done for each individual subshell and each projectile charge-state separately. For slow heavy particles, however, electron-exchange and dynamic mean-field effects will be important and have to be incorporated in the treatment. The use of time-dependent Hartree-Fock methods might be necessary for this purpose. There is also a need for density-functional methods which are applicable to finite projectile velocities. At this point it should be emphasized once again that there is no strictly non-perturbative model which may be applied to the prediction of the impact-parameter dependence of the energy loss of channeled ions in metals.

This work shows the possibility of performing first principle (coupled-channel) calculations for the energy loss problem. The results give deeper insights into the basic energy transfer mechanisms and their importance with respect to impact parameter and incident energy.

Acknowledgments

One of the authors (P.L.G.) would like to acknowledge the Alexander von Humboldt Foundation (Germany), CNPq (Brazil) and Hahn-Meitner Institut (Berlin) for the financia1 support.

References

1. P. M. Echenique, R. M- Nieminem and R. H. Ritchie, Solid State Commun. 37, 779 (1981).

2. P. M. Echenique, R. M- Nieminem, J. C. Ashley and R. H. Ritchie, Phys. Rev. A33, 897 (1986).
3. N. M. Kabachnik, V. N. Kondratev and O. V. Chumanova, Phys. Stat. Sol(b) 145, 103 (1988).
4. C. Auth and H, Winter, Phys. Lett. **A176**, 3055 (1993).
5. H. H. Mikkelsen and P. Sigmund, Nucl. Instr. and Meth. **B27**, 266 (1987).
6. H. H. Mikkelsen and P. Sigmund, Phys. Rev. **A40**, 101 (1989).
7. L. C. Northcliffe and R. F. Schilling, Nucl. Data Tables 7, 233 (1970).
8. The Stopping and Ranges *of Ions* in Matter, edited by H. Andersen and J. F. Ziegler (Pergamon, New York, 1977) vol 3.
9. F. Janni, At. Data Nucl. Tables 27, 147 (1982).
10. J. F. Ziegler, J. P. Biersack and U. Littmark, The Stopping and Ranges of *Ions* in Solids, (Pergamon, Oxford, 1985), vol 1.
11. O. B. Firsov, Sov. Phys. - JETP 9, 1076 (1959).
12. J., Lindhard, Mat. Fys. Medd. Dan. Vid. Selsk. 28: no. 8, (1954); J. Lindhard and M. Scharff, Phys. Rev. 124, 128 (1961); J., Lindhard, M. Scharff, and H.E. Schiott, Mat. Fys. Medd. Dan. Vid. Selsk. 33: no.8, (1963).
13. P. L. Grande and G. Schiwietz, Phys. Lett. **A163**, 439 (1992).
14. F. Flores in Interaction of Charged *Particles* with Solid and Surfaces, edited by A. Grass-Marti, H. M. Urbassek, N. R. Arista and F. Flores, NATO ASI Series, Series B: Physics Vol. 271 (Plenum Press, New York).
15. K. Dettmann, Z. Phys. **A272**, 227 (1975).
16. V. A. Khogyrev and E. I.Sirotinin, Phys. Stat. Sol. (b)**116**, 659 (1983).
17. J. Lindhard and A. Winter, K. Dan. Vidensk. Selsk. Mat.-Fys. Medd. 24, No. 4 (1964).
18. E. Bonderup, K. Dan. Vidensk. Selsk. Mat.-Fys Medd. 35, No 17 (1967).
19. K. B. Winterbon, Rad. Effec. 79, 251 (1983).
20. H. Ascolani and N. R. Arista, Phys. Rev. A33, 2352 (1986).
21. H. H. Mikkelsen and P. Sigmund, Phys. Rev. **A40**,101 (1989).
22. G. Schiwietz, Phys. Rev. A42, 296 (1990).
23. P. L. Grande and G. Schiwietz, Phys. Rev. A44, 2984 (1991).
24. G. Schiwietz and P. L. Grande, Nucl. Instr. and Meth. B69, 10 (1992).
25. P. L. Grande and G. Schiwietz, Phys. Rev. **A47**, 1119 (1993).
26. G. Schiwietz and P. L. Grande, Rad. Eff. and Def. in Solids, Vol. 27 in press.
27. G. Schiwietz and P. L. Grande, Nucl. Instr. and Meth., in press (1994).
28. J. J. Dorado and F. Flores, Phys. Rev. **A47**, 3092 (1993).
29. P. Bauer, F. Kastner, A. Arnau, A. Salin, P. D. Fainstein, V. H. Ponce, and P. M. Echenique, Phys. Rev. Lett. 69, 1137 (1992).
30. L. L. Balashoval N. M. Kabachnik and V. N. Kondratev, Phys. Stat. Sol (b) 161, 113 (1991).
31. J. Bang and J. M. Hansteen, Kgl. Dan. Vidensk. Selsk. Mat. Fys. Medd. 31, No.13 (1959); L. Wilets and S. J. Wallace, Phys. Rev. 169, 84 (1968); M. R. Flannery and K. J. MacCann, Phys. Rev. **A8**, 2915 (1973).
32. F. Herman and S. Skillmann, in Atomic Structure Calculations, (Prentice-Hall, New Jersey, 1963).
33. A. Dalgarno and G. W. Griffing, Proc. Roy. Soc. **A232**, 423 (1955); G. H. Gillespie and M. Inokutti, Phys. Rev. **A22**, 2430 (1980).
34. M. Moneta, J. Phys. B (1994), to be published.
35. A. Arnau, M. Penalba, P. M. Echenique, F. Flores and R. H. Ritchie, Phys. Rev. Lett. 65, 1024 (1990).
36. T. Kaneko, Phys. Rev. A33, 1602 (1986).
37. D. R. Bates and G. W. Griffing, Proc. Phys. Soc. A68, 90 (1955).
38. E. C. Montenegro, W. E. Meyerhof and J. H. McGuire, Advances in Atomic Mol. and Opt. Phys., vol 33 (1994) in print; E.C. Montenegro and W. E. Meyerhof, Phys. Rev, **A43**, 2289 (1991); J. H. McGuire, N. Stolterfoht and P. R. Simony, Phys. Rev. A24, 97 (1981).
39. M. Abramowitz and I. Stegun, *Handbook* of Mathematical Functions (Dover, New York, 1970).
40. O. G. Larsen and K. Taulberg, J. Phys B: At. Mol. Phys. 17, 4523 (1984).
41. G. Baur, M. Pauli and D. Trautmann, Nucl.Phys. **A211**, 333 (1974).

42. D. R. Bates and G. Griffing, Proc. Phys. Soc. **A66**, 966 (1953).
43. O. Oer and M. Robinson, Nucl. Instr. and Meth. 132, 647 (1976).
44. H. A. Bethe, R. W. Jackiw, *Intermediate Quantum Mechanics* (W. A. Benjamin, New York, 1968), 2nd edition.
45. N. Bohr, Philos. Mag. 25, 10 (1913), N. Bohr, K. Dan. Vidensk. Selsk. Mat.-Fys. Medd. 18, No. 8 (1948)
46. B. Skogvall and G. Schiwietz, Phys. Rev. Lett. 65, 3265 (1990).
47. G. Schiwietz, in Ionitation of Solids by Heavy *Particles*, edited by R. A. Baragiola, (Plenum Press, New York, 1993).
48. S. K. Allison, Rev. Mod. Phys. 30, 1137 (1958).
49. H. K. Reynolds, D. N. F. Dunbar, W. A. Wenzel, and W. Whaling, Phys. Rev. 92, 742 (1953).
50. J. A. Phillips, Phys. Rev. 90, 532 (1953); (d and t projectiles were used for incident energies below 40 keV).
51. P. K. Weyl, Phys. Rev. 91, 289 (1953).
52. J. T. Park and E. J. Zimmermann, Phys. Rev. 131, 1611 (1963).
53. F. Besenbacher, H. H. Andersen, P. Hvelplund and H. Knudsen, Mat. Fys. Medd. Dan. Vid. Selsk. 40: no.3, (1979).
54. R. Golser and D. Semrad, Phys. Rev. Lett. 66, 1831 (1991) (d and p projectiles were used).
55. E. Bonderup and P. Hvelphlnd, Phys. Rev. **A4**, 562 (1971).
56. S. D. Warshaw, Phys. Rev. 76, 1759 (1949).
57. R. A. Langley, Phys. Rev. **B12**, 3575 (1975).
58. M. Kimura, Phys. Rev. **A47**, 2393 (1993).
59. P. Sigmund, Phys. Rev. **A14**, 996 (1976).
60. Besenbacher, J. U. Andersen and E. Bonderup, Nucl. Instr. and Meth. 168, 1 (1980).
61. F. Besenbacher, H. H. Andersen, P. Hvelplund and H. Knudsen, K. Dan. Vidensk. Selsk. Mat.-Fys. Medd. 40, No. 9 (1981).
62. P. Hvelplund K. Dan. Vidensk. Selsk. Mat.-Fys. Medd. 38, No. 4 (1971).
63. P. L. Grande, F. C. Zawislak, D. Fink, and M. Behar, Nucl. Instr. and Meth., **B61**, 282 (1991).